ICARUS 22, 24–47 (1974)

Variable Features on Mars. IV. Pavonis Mons[1]

CARL SAGAN AND J. VEVERKA[1]

Laboratory for Planetary Studies
Cornell University
Ithaca, New York 14850

R. STEINBACHER

Jet Propulsion Laboratory
California Institute of Technology
Pasadena, California 91109

AND

L. QUAM, R. TUCKER, AND B. EROSS

Artificial Intelligence Laboratory
Stanford University
Stanford, California 94305

Received November 13, 1973; revised January 7, 1974

A remarkable set of albedo changes has been uncovered by Mariner 9 photography of the upper slopes of the shield volcano Pavonis Mons, near its summit caldera. The most likely explanation of the event is aeolian transport of fine-grained particles. Since the atmospheric pressure in this locality is $\sim$1.5 mb, minimum wind velocities above the surface boundary layer of about 110 m/s are necessary, corresponding to 0.51 of the speed of sound. Slope winds in this velocity range are expected near the upper flanks of major Martian volcanic constructs.

I. Introduction

In previous papers (Sagan *et al.*, 1972, 1973; Veverka *et al.*, 1974), we have outlined the general character of the surface albedo variations uncovered on Mars during the course of the Mariner 9 mission and in the time between the Mariner 6 and 7 and the Mariner 9 missions. We have presented evidence that the bulk of these surface variations are due to windblown sand and dust, and that the classical groundbased observations of seasonal and secular changes are the same phenomenon but seen under low resolution. The present paper is the first of several to examine specific Martian regions in which changes were observed during the course of the Mariner 9 mission.

Shortly after insertion into Mars orbit, on November 14, 1971, Mariner 9 observed four dark spots in the Tharsis region which —apart from the South Polar Cap—were the only surface features visible near the time of maximum intensity of the great 1971 global dust storm. As the storm decayed, it became clear that these four spots were each enormous volcanic mountains with summit calderas (Masursky *et al.*, 1972; McCauley *et al.*, 1972).

The low albedo of the Tharsis shield volcanoes is open to two possible explanations: in terms of composition and particle size. These volcanoes are thought to be relatively young (Hartmann, 1973) and basaltic. There may have been inadequate time for the oxidation and weathering of the basic rocks which constitute these volcanoes into brighter more oxidized material which characterizes the surrounding lowlands. On the other hand

[1] Paper presented at the International Colloquium on Mars, 28 November–1 December 1973, Pasadena, California.

the slopes of several degrees of these shield volcanoes and their high altitudes lead to very high speed slope winds (Gierasch and Sagan, 1971; Sagan *et al.*, 1971) which may keep their flanks free of fine bright particles. The latter process must certainly be operative since the lowest flanks of the volcanoes were below the top of the 1971 dust cloud. Therefore, following each major duststorm these slopes must be subject to bright particle fallout, and must subsequently be swept clean by winds if they are to remain dark relative to their surroundings between major duststorms.

The present paper is devoted to changes observed in Pavonis Mons, a volcanic mountain at latitude, 113°W, longitude, 1°N, previously known informally as Middle Spot. The official IAU name Pavonis Mons intentionally elicits the small classical dark albedo feature Pavonis Lacus, to which it corresponds in position reasonably well. According to Antoniadi (1929) Pavonis Lacus exhibits secular variations, being more prominent at some oppositions than at others.

II. Changes on the Slopes of Pavonis Mons

An oblique view of the upper portions of Pavonis Mons can be seen in Fig. 1. The entire volcano is some 400 km across. The summit caldera is about 50 km wide,

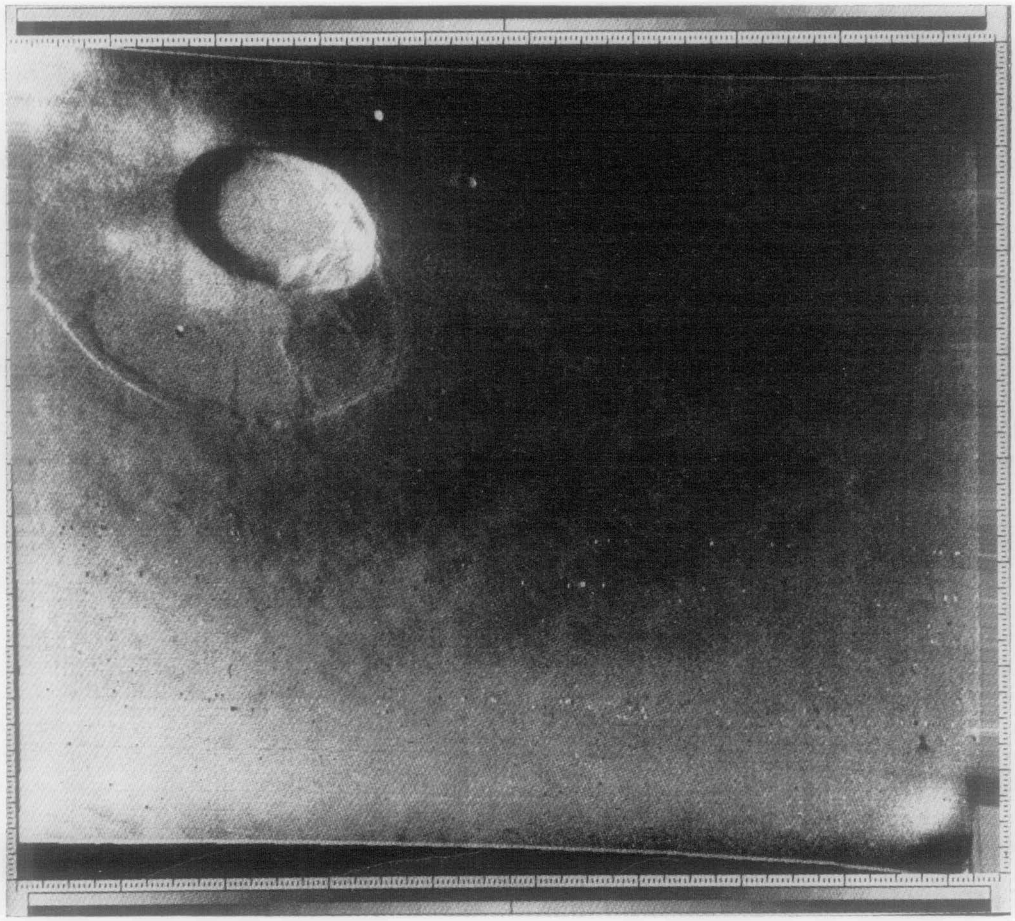

FIG. 1. Oblique view of Pavonis Mons taken by Mariner 9 on Revolution 65. The base of the volcano and the surrounding lowlands are still obscured by atmospheric dust associated with the waning stages of the 1971 duststorm. The summit caldera is about 50 km across. (DAS 03930230; IPL 976/240831).

TABLE I

SUMMARY OF PAVONIS MONS COVERAGE

Revolution	Day number	Calendar day	$L_s(°)$
65	350	16 Dec. 71	311
78	356	22 Dec. 71	315
117	11	11 Jan. 72	326
152	28	28 Jan. 72	336
154	29	29 Jan. 72	336
195	50	19 Feb. 72	347
232	68	8 Mar. 72	356

and, judging from the length of the shadow of its inner wall, several kilometers deep. Table I summarizes the Mariner 9 photography of Pavonis Mons utilized in this study.

In Fig. 2 is a comparison of two views of the summit caldera of Pavonis Mons, rectified and scaled at the Artificial Intelligence Laboratory of Stanford University. Subsequent picture comparisons in this paper have been similarly prepared at Stanford. The process is described by Levinthal *et al.* (1972) and by Quam *et al.* (1973). Figure 2 is a comparison of a frame obtained with an orange filter on Revolution 78 with a frame obtained with a polarizing orange filter on Revolution 154. The transmission passbands of the two filters are negligibly different, and the two pictures were taken with comparable photometric angles. The low contrast in the Revolution 78 view can be attributed almost entirely to the presence of atmospheric dust associated with the 1971 duststorm.

In Fig. 3, which is a comparison between Revolutions 154 and 195, striking localized darkenings to the north and east of the summit caldera are revealed. Figure 4A is a comparison between the frame taken on Revolution 195 and a frame taken on Revolution 232. Unlike the last two comparisons, the lighting angles are significantly different here. In addition certain topographic features such as the northeast circumferential ridge are indistinct in the Rev. 232 view. This makes it very difficult to align the two views precisely—and, as the different outlines of the caldera in the two views indicate, the alignment is indeed only approximate. The general loss of surface topographic details could be attributed to condensate haze or clouds in this region on Revolution 232. However, as discussed in Section III, high resolution frames taken on the same orbit (Figs. 5 and 6) show a wealth of topographic and albedo detail. It therefore seems that the apparent loss of detail in the Rev. 232 A-frame (Fig. 4 and Fig. 8 below) is entirely due to non-optimum lighting conditions and to increased transmission noise. The Revolution 232 frame was taken with the sun only 24 degrees from the zenith, whereas in the other frames used in Figs. 2, 3 and 4, the sun is 50° to 60° from the zenith enhancing shadows and making topographic detail more evident.

Fortunately high resolution B-frame imagery of these changes is also available. Figure 5 is a B-frame view of the caldera and upper flanks of Pavonis Mons showing the albedo markings in question. Two views of the region of one of these markings is shown in Figs. 6A and B. In Fig. 6A the albedo marking is absent, although topographic detail stands out crisply; in Fig. 6B the dark patch is present. Combining the information in Figures 3 and 6, we conclude that this albedo patch appeared sometime between Rev. 154 and Rev. 195, and was still there on Rev. 232.

Before dealing with other less well documented changes in this area, we will try to explain the above albedo change in some detail.

III. POSSIBLE EXPLANATIONS

Just as with the explanation of the general low albedo of Pavonis Mons there are two categories of possible explanations for the albedo variations: explanations in terms of composition, and explanations in terms of particle size. One natural compositional explanation is that the darkenings represent the venting of volcanic ash. A 20-day time scale for development of such a flow is perfectly consistent with terrestrial ashflows (Macdonald, 1971). A lower

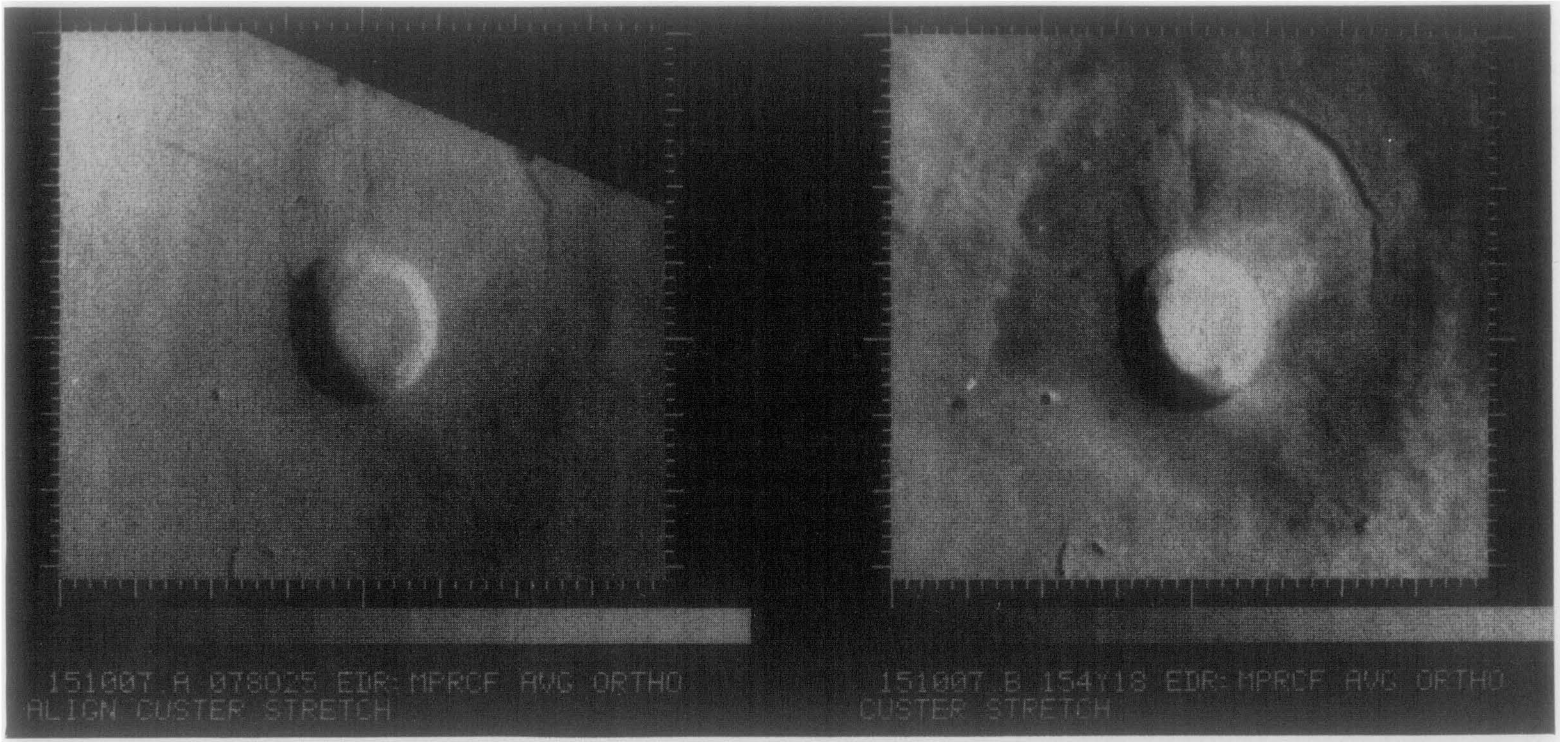

FIG. 2. Two views of the summit of Pavonis Mons. Left: Revolution 78; Right: Revolution 154. The low contrast at left is due to atmospheric dust associated with the waning stages of the 1971 duststorm. By Revolution 154, the atmosphere was clear and both topographic and albedo details are visible on the flanks of Pavonis Mons. In this and other Stanford picture products in this paper, the smallest division of the border scales represents 5 picture elements (pixels). Here the scale, $K = 1.09$ km/pixel. (STN: 151007).

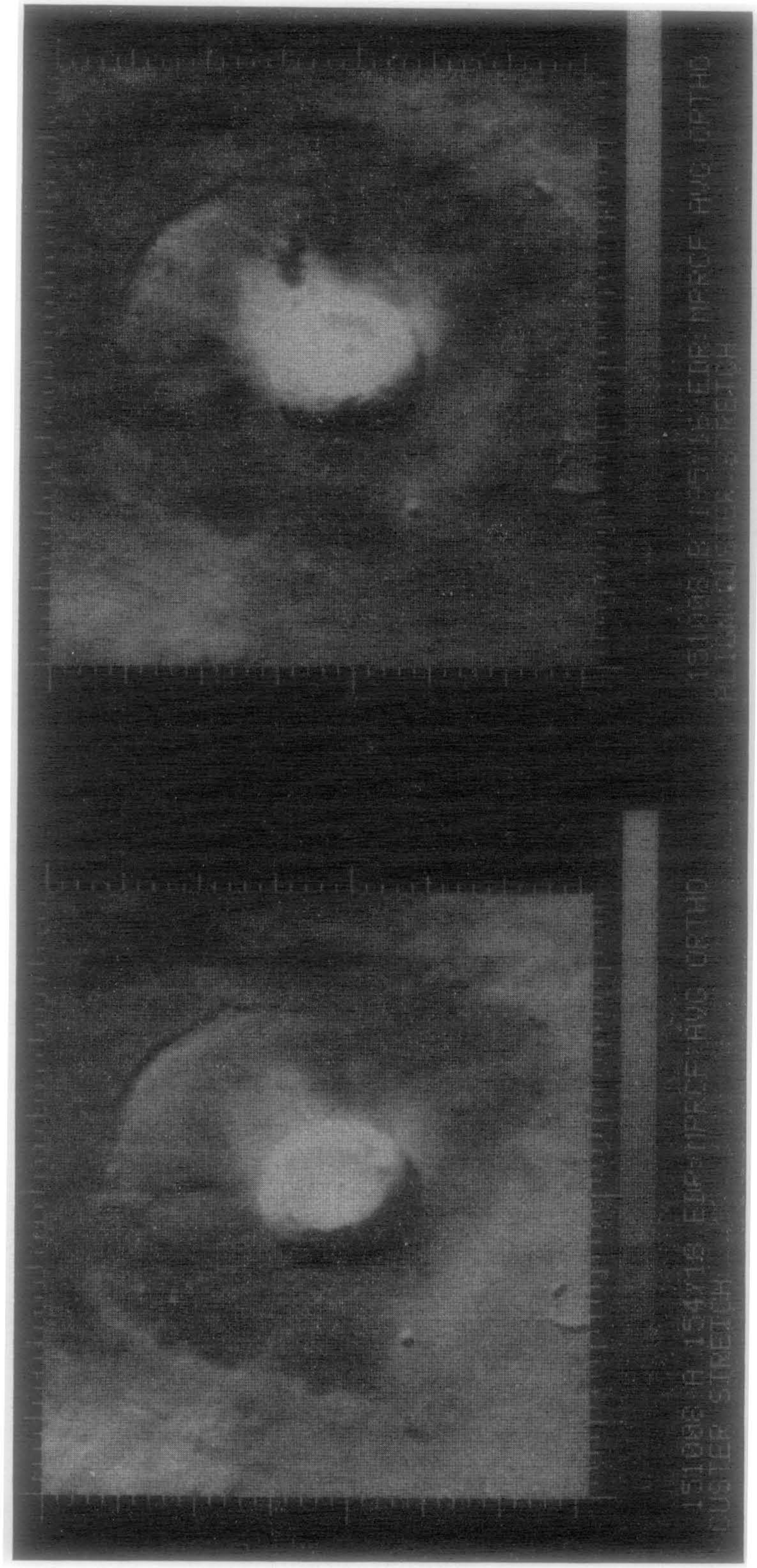

FIG. 3. Pavonis Mons. Left: Revolution 154; Right: Revolution 195. Note the appearance of at least three prominent dark albedo markings on the slopes near the caldera during this 20 day interval. (K = 1.09, STN: 151008).

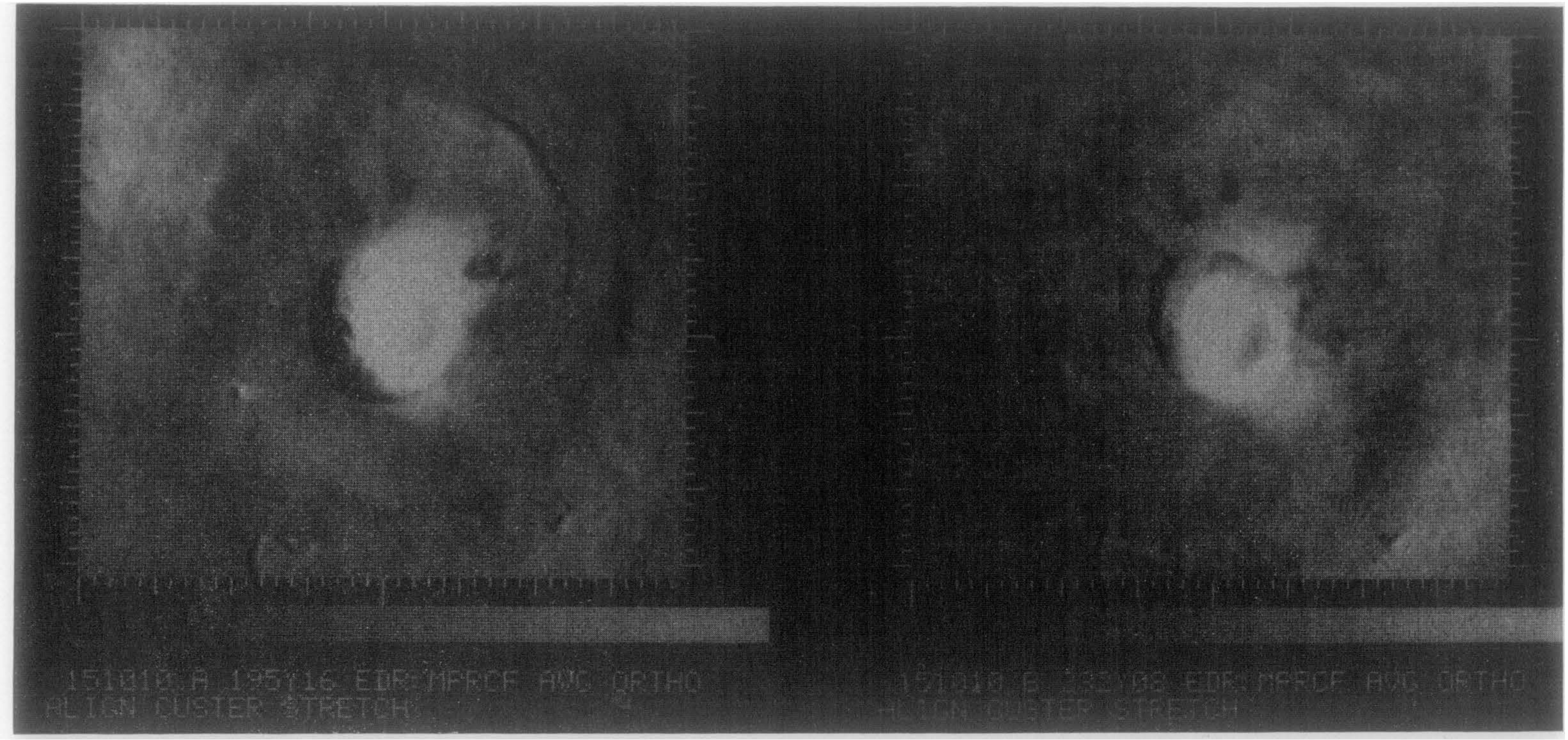

FIG. 4. Pavonis Mons. (a). Left: Revolution 195; Right: Revolution 232. The photometric geometry (lighting, viewing, and phase angles) differ significantly between left and right. Whereas the views on the left were obtained under low sun conditions (50°–60° from the zenith), the sun is almost vertical (24°) on the left. These high sun conditions lead to a loss of detail and make registration of the views on the left and right difficult. Apparent albedo variations must be interpreted with caution. Many, such as the appearance of the two bright patches near the rim of the caldera on Revolution 232, are almost certainly due to the significant differences in photometric geometry. It is argued in the text that the loss of detail on the left is not likely due to the presence of clouds since high resolution frames taken on the same orbit (Figs. 5 and 6) show a wealth of albedo and topographic detail. ($K = 1.09$ km/pixel; STN 151009/10).

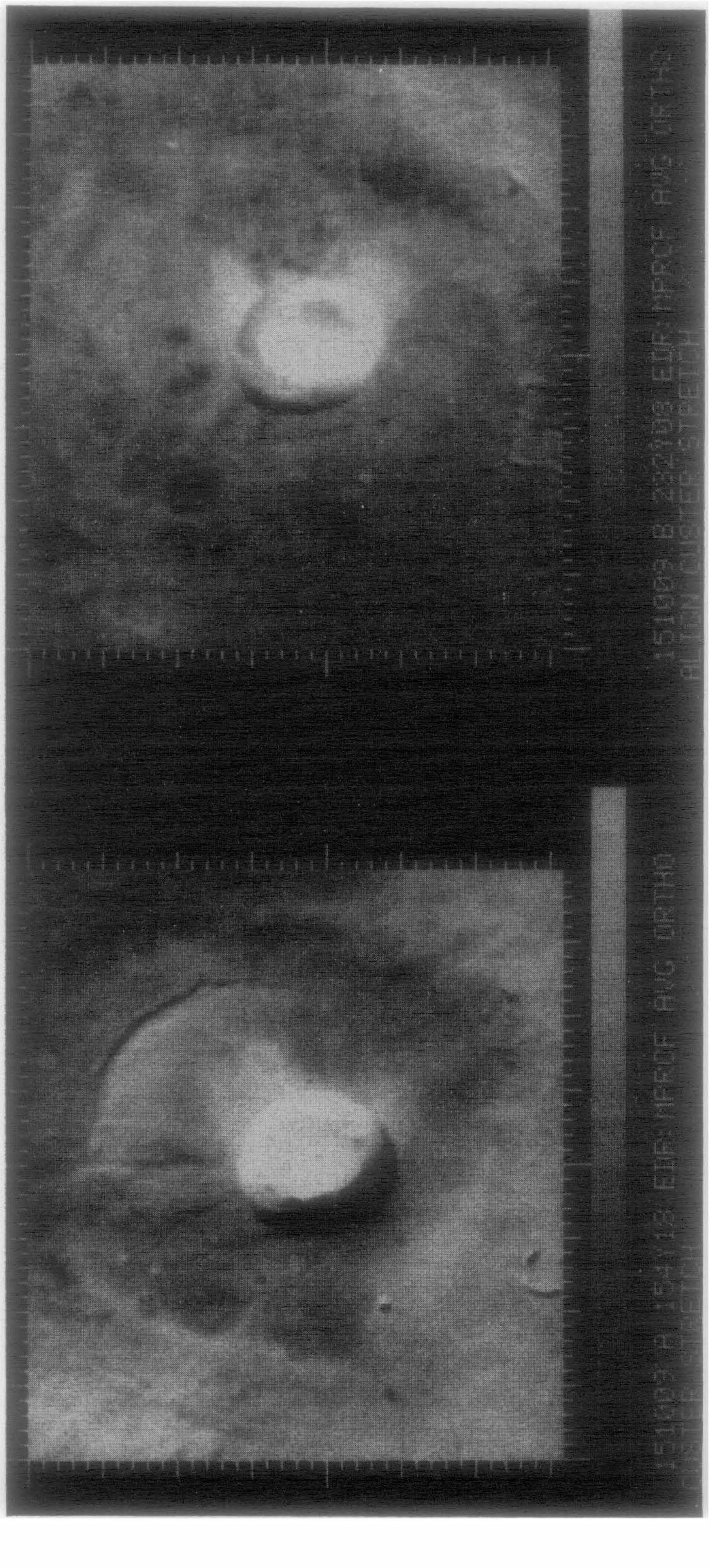

Fig. 4. Pavonis Mons. (b). Left: Revolution 154; Right: Revolution 232.

limit to the thickness of putative ash, as seen on Revolution 232, Fig. 5, is perhaps 1 mm. The corresponding mass of ash needed to produce the three dark splotches near the summit caldera would then be $\sim 10^{13}$ grams. Terrestrial ash flows involving masses 10^4 times this large are not uncommon (Macdonald, 1971, p. 159), and in this interpretation the changes detected on the upper slopes of Pavonis Mons correspond to a very minor ash flow. Of course 1 mm thickness is a low lower limit and a mass of flowing ash comparable to large terrestrial ash flows would also be consistent with the observations. However, there is no morphological evidence that these events are due to the venting of volcanic ash. There are no obvious vents along or near the radial ridges. Carr (1973) also believes that the appearance of these splotches is inconsistent with a volcanic origin—either ash venting or lava flow.

Added to this is the fact that some mechanism other than ash venting must be active on Pavonis Mons to explain the secular changes reported by Antoniadi (1929). It seems unlikely that each change in appearance seen from Earth is caused by a particular ash venting event. Even in such a case the subsequent aeolian redistribution of dark ash or aeolian covering by bright dust is required if a permanent darkening of Pavonis Mons is to be avoided. Given this fact, one must consider the obvious alternative that a purely aeolian explanation is sufficient.

We now show that the changes displayed in Figs. 2, 3 and 6 can be understood by the removal of fine bright dust by winds. At the conclusion of the argument we briefly discuss the origin of this bright dust.

In previous papers in this series we have outlined a range of evidence for particle transport by high speed winds on Mars, and have stressed that aeolian particle size segregation of material of fixed composition will lead to changes in albedo.

The albedo changes on Pavonis Mons occur very close to the summit. At least four sources of data on the elevation profile of Pavonis Mons exist. According to data from the Mariner 9 ultraviolet spectrometer (Hord, 1974), the rim of the caldera is at an altitude of 14 to 19 km above the 6.1 mb pressure level. On this scale, the western base of this volcanic construct is at an altitude of about 10 km; the eastern base at roughly 6 km. With the scale height used in Hord's reduction, the corresponding pressure near the summit is 1.3 to 2.0 mb. From photography with the Mariner 9 TV system, Blasius (1973) deduces a relief $\sim$10 km above the western base of Pavonis Mons, in substantial agreement with the UVS results. The infrared interferometric spectrometer aboard Mariner 9 observed only the flanks of Pavonis Mons; the resulting upper limit on the summit pressure (Conrath *et al.*, 1973) is about 3.0 mb. By luck the S-band transmitter of Mariner 9 was occulted by Pavonis Mons on the nadir pass of Revolution 434 (Kliore *et al.*, 1973), yielding a pressure somewhere on the upper flanks of the volcano of 1.0 mb. The S-band occultation experiment measures the altitude of the highest point along the line of sight between the spacecraft and the Earth. If this occultation point was not the very summit of Pavonis Mons, then the summit pressure may be even less than 1.0 mb. The S-band occultation measurement is more direct and perhaps more reliable than measurement made by other methods. In the following discussion, we adopt a pressure of 1.5 mb for the region of albedo variations shown in Figs. 5 and 6. Since it is the two-thirds root of the pressure which will be involved in the discussion below, high accuracy for this pressure is not required.

What is the connection between local topography and these albedo changes? According to the UVS topography of Pavonis Mons (Hord *et al.*, 1974), the highest elevations occur along the circumferential ridge (Fig. 2). The southwestern rim of the caldera (lowest left rim in Fig. 2), which is tangent to the prolongation of the circumferential ridge, may be 2–4 km higher than the northeastern rim (upper right rim in Fig. 2) of the caldera. Thus the changes in question occurred within a large summit depression outlined in part by the circumferential ridge. This is consistent with the coarser topographic

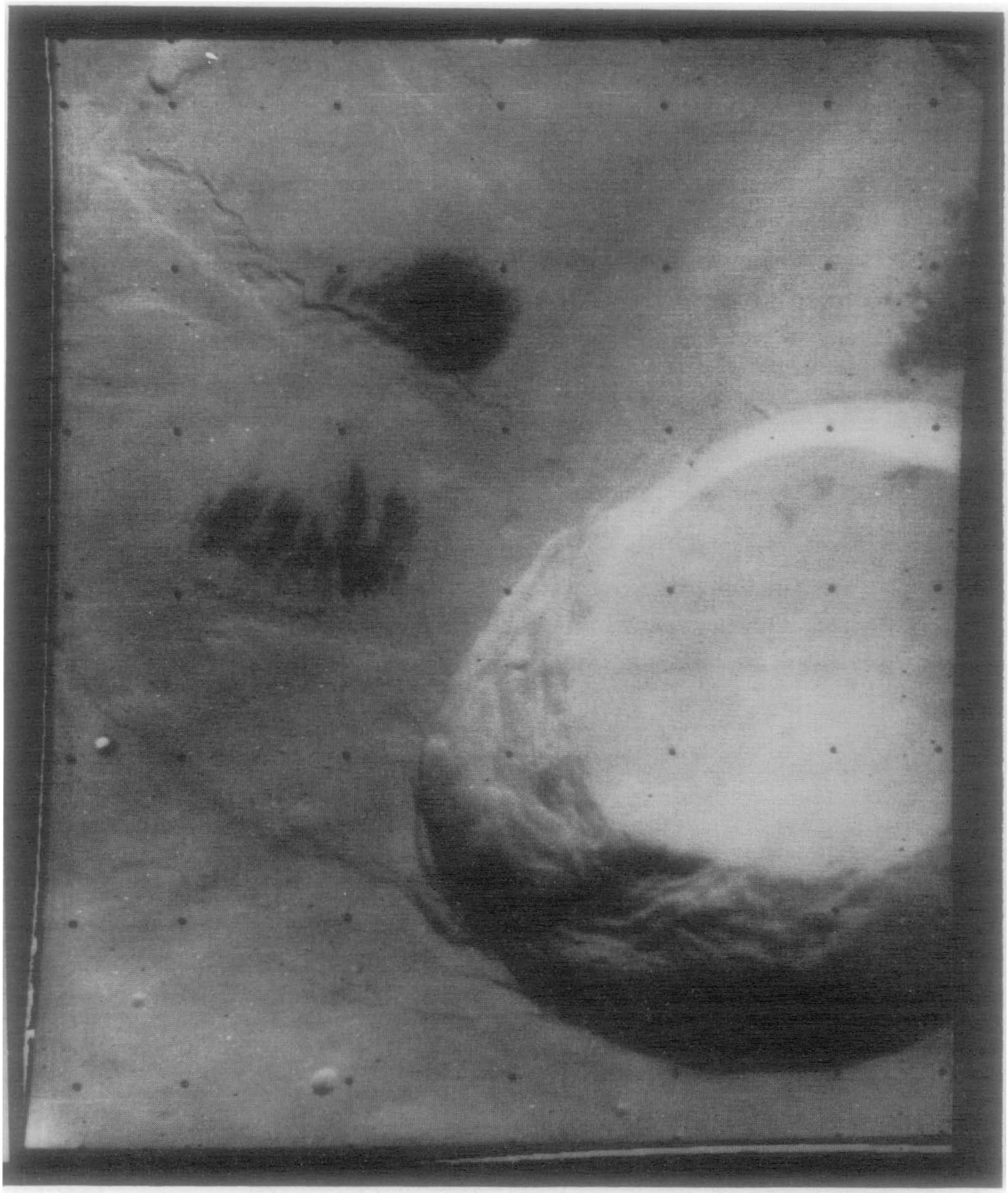

FIG. 5. Two high resolution views of the Pavonis Mons summit taken on Revolution 232. At top, two of the large dark albedo patches which appeared between Revolutions 154 and 195 (Fig. 3) are seen at upper right. Part of the third patch is seen near the bottom edge to the right of the caldera. Note several dark albedo markings on the floor of the caldera. Approximate width = 100 and 120 km respectively. (DAS 09917259/329).

profile of Pavonis Mons derived by Blasius (1973) from photogrammetry. It is also consistent with high resolution photography (Figs. 5A, B) which shows that the western wall of the caldera (left wall in Fig. 5A) is considerably deeper than the eastern wall (right wall in Fig. 5A). Specifically, with reference to Fig. 5B, this means that the highest elevations are reached along the outer ridge which circum-

FIG. 5 (*Cont'd*).

scribes a summit area which in places is 2–4 km lower than this ridge. The changes discussed occur on the downslope of this summit depression at the top of Pavonis Mons. Part of this depression is occupied by the caldera. Another view of the topography, after the UVS results of Hord, *et al.* (1974) is given in Fig. 7, where the location of the eastern dark patch of Fig. 3 on an upslope between the caldera and the circumferential ridge can be deduced.

The albedo change in Fig. 6 appears to be connected intimately with the radial wrinkle ridge which extends down the flank of Pavonis Mons and into the circumferential ridge. Figure 5 suggests that

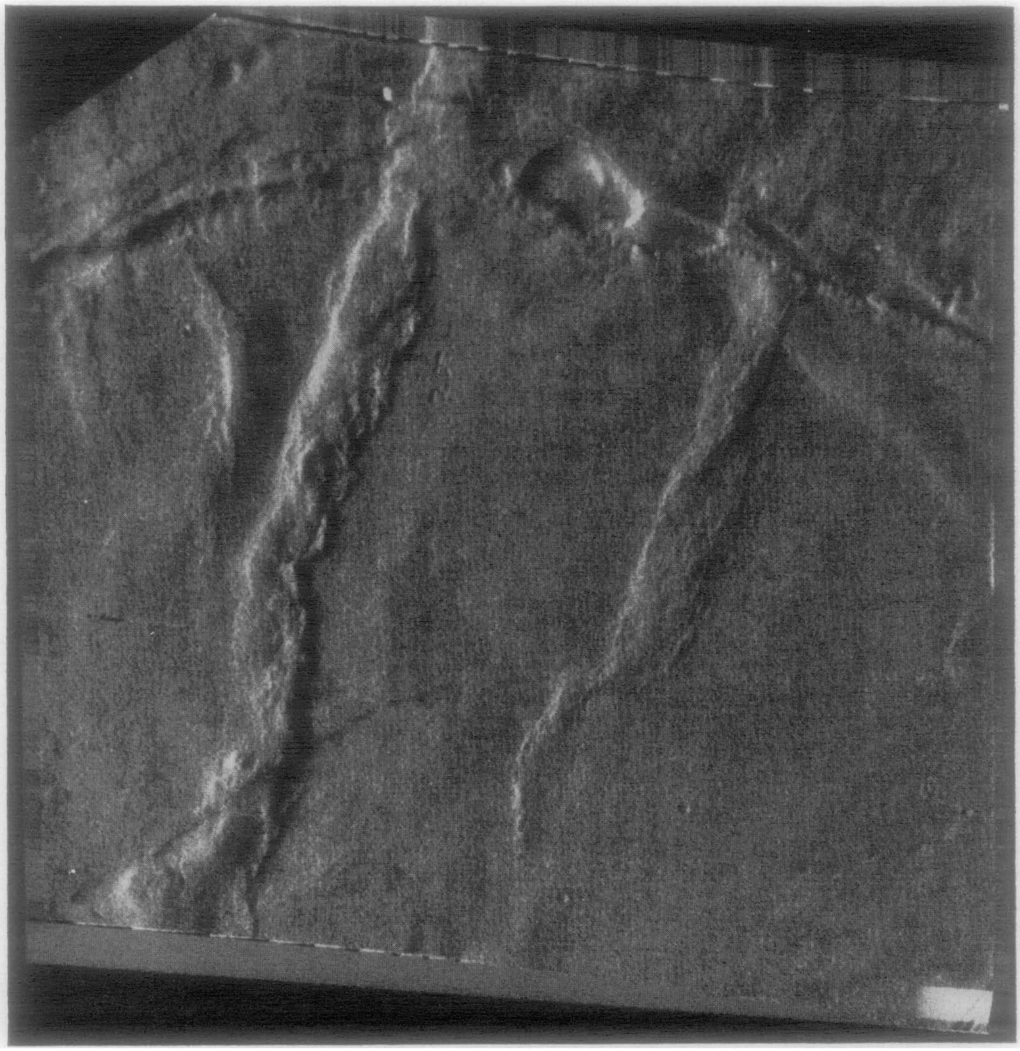

FIG. 6. One of the changes in Fig. 3 seen with the high resolution camera. Left: Revolution 78; Right: Revolution 232. Transmission noise, negligible in the left view, is considerable in the view on the right, due mostly to increased spacecraft–Earth separation. Approximate width = 50 km. (DAS 04402170: IPL 212240 and DAS 09917329: IPL 142634)

the other albedo change, about 15 km to the west, is also associated with a ridge. This is perhaps more evident from a close study of Fig. 3. Other instances of apparent connection between albedo changes and local topography, especially ridges, have been noted in other areas of Mars (Sagan *et al.*, 1972). Especially striking is the fact that the albedo change occurs almost in contact with the steepest part of the ridge. The scalloped appearance of the dark albedo areas (which are about 10×10 km in extent) indicate the effects of winds, and mark these locations as regions of increased wind velocity.

From the arguments of Bagnold (1941) it follows that the threshold frictional velocity, V_{*t}, necessary to initiate grain motion at the surface is proportional to $\rho^{-2/3}$, where ρ is the atmospheric density (Sagan and Pollack, 1967). The threshold frictional velocity, V_{*t}, at the 5 mb surface in the Martian atmosphere necessary for grain motion is 2.6 ± 0.2m/s

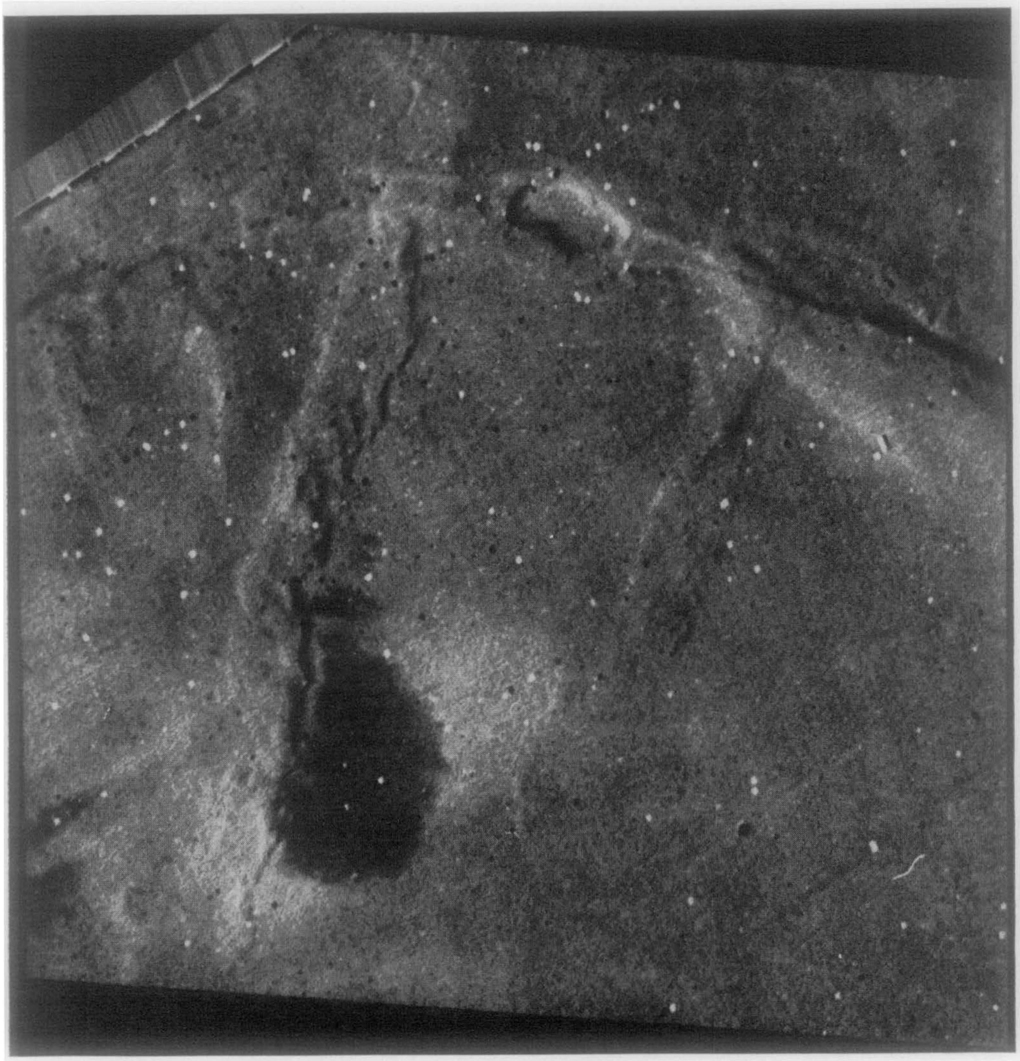

FIG. 6 (*Cont'd*).

(Hess, 1973; Greeley *et al.*, 1973; Sagan and Veverka, 1974). The corresponding value at the 1.5 mb pressure level is then 6 m/s. There is a range of estimates of $\chi \equiv V_{gt}/V_{*t}$, the ratio of the velocity above the boundary layer to the corresponding surface frictional velocity (Sagan and Veverka, 1974); by far the lowest value is that of Gierasch and Goody (1973): $\chi = 18$, corresponding to $V_{gt} = 110$ m/s.

We have noted that the major albedo changes on Pavonis Mons occurred adjacent to wrinkle ridges, which are possibly locales of enhanced local roughness. Golitsyn (1973) estimates that V_{*t} may be decreased by as much as 30% in very rough regions. This corresponds to $V_{gt} > 75$ m/s. If such topographic effects are involved, they may help explain why only a fraction of the upper flanks of Pavonis Mons were observed to darken. But higher values of χ lead to $V_{gt} > 110$ m/s, even with effects of roughness included.

The atmospheric temperature near the summit of Pavonis Mons was measured by the S-band occultation experiment (Kliore *et al.*, 1973) as 209°K. Because of the inefficient heat exchange between atmosphere

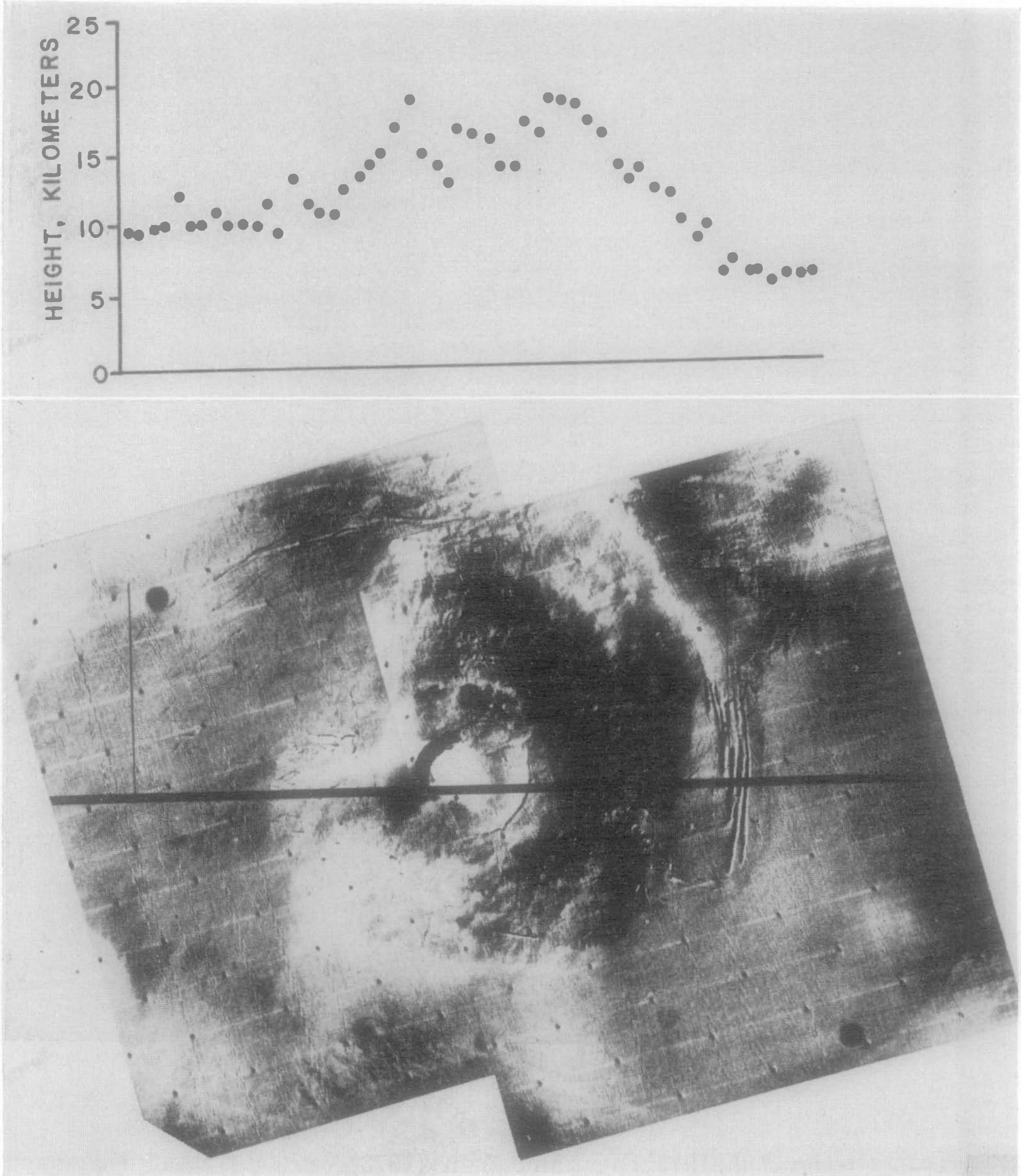

FIG. 7. A vertical view of Pavonis Mons, showing the lower circumferential graben well and the upper circumferential ridge poorly, compared with the UVS elevation profile along a pass through the summit caldera, as shown. After Hord *et al.* (1974).

and ground at these low densities, this should be a characteristic temperature above Pavonis Mons during the observed changes. With this temperature, $V_{gt} =$ 110 m/s corresponds to a minimum Mach number of about 0.51.

It is likely that Mach numbers as large as unity are excluded in planetary meteorology by a variety of dissipative processes. This requirement sets a limit $\chi \lesssim 36$ in the vicinity of Pavonis Mons. This is an interesting restriction, since most models of the boundary layer physics for Mars yield results in the range $45 \leqslant \chi \leqslant 30$ (Sagan and Veverka, 1974). Very high winds are to be expected on the slopes of volcanic constructs like Pavonis Mons (Gierasch and Sagan, 1971).

The explanation offered here is that the changes shown in Figs. 3, 5 and 6, are due to the aeolian removal of a layer of bright wind transportable material, and the exposure of an underlying, darker and more wind-resistant layer. The boundaries of the dark markings which appeared between Revolution 154 and 195 are in part jagged and streaky, and characteristic of aeolian phenomena (Sagan *et al.*, 1973).

An obvious source of the bright material is the 1971 dust cloud, implying that this cloud must have reached pressure levels of less than 1 mb at some time. Independent evidence that the dust cloud reached even higher altitudes exists (Parkinson and Hunten, 1972). It is true that the albedo variations of Figs. 3, 5 and 6 are also explicable by aeolian transport of dark particulates, if a plausible source of such low albedo material could be found. But in this case a source of dark particulates is not evident, while a source of bright wind-transportable particles can be demonstrated to exist.

IV Other Changes

Figures 8 and 9 provide comprehensive views of the Pavonis Mons volcano and its surroundings, showing the prominent circumferential grabens at its base (Carr, 1973) and a series of radial channels (conceivably old lava tubes) on the eastern flanks. The graben system is well below the altitude of the circumferential scarp shown in Figs. 2–6. The low albedo of Pavonis Mons relative to its surroundings is clearly brought out in Fig. 8.

There is a striking difference between the general aspect of Pavonis Mons in Figs. 8 and 9. Much topographic detail, clearly visible in Fig. 8, is vague or absent on Fig. 9, one example being the circumferential scarp. Both groundbased and spacecraft observations (Leovy *et al.*, 1972) show that the Tharsis volcanoes have frequent slope and summit clouds which are probably orogenic, but which just possibly may partly be due to volcanic outgassing.

We have argued above that this apparent loss of detail in Fig. 9 must be due largely to the high sun conditions under which this frame was taken, and not to the presence of clouds, since high resolution frames in this area taken on the same orbit show no evidence of such clouds (Figs. 5 and 6).

There are several other striking differences between the albedo patterns in Figs. 8 and 9. These enigmatic changes can be divided into three categories. Referring to Fig. 9, we see first on the left an apparent intense darkening just below the circumferential graben system and trending parallel to it. Second, at the western base of the volcano there is a contiguous series of short dark radial splotches running for about 90° around the base of the volcano. Third, to the east and southeast the base of the volcano shows a series of long dark radial streaks, some of which are about 200 km in length.

It is conceivable that the first two of these changes are due to the presence of clouds. The areas in question may appear dark because their surroundings are covered by bright clouds. In addition some of the smaller dark splotches could conceivably be cloud shadows.

Since we do not have high resolution frames of this portion of Pavonis Mons we cannot argue conclusively against clouds in this region on Revolution 232, as we can in the case of the areas covered by Fig. 5. Neither, however, can we argue that these changes are not true surface albedo changes of the same type as seen in Figs. 5 and 6. The very dark albedo area in line with the graben system (Fig. 10, right) is easier to explain. There is no evidence for clouds in its vicinity, and it is likely a true surface albedo change.

Finally, in Fig. 11 we show a series of picture comparisons of the third area of interest noted above. Significant changes have occurred between Revolution 195 and 232. From their appearance these long dark streaks running radially down the volcano appear to be surface albedo features. Referring back to Figs. 9 where the full extent of this pattern of dark streaks is evident, we find it difficult to see how such a pattern could be produced by clouds or cloud shadows, but

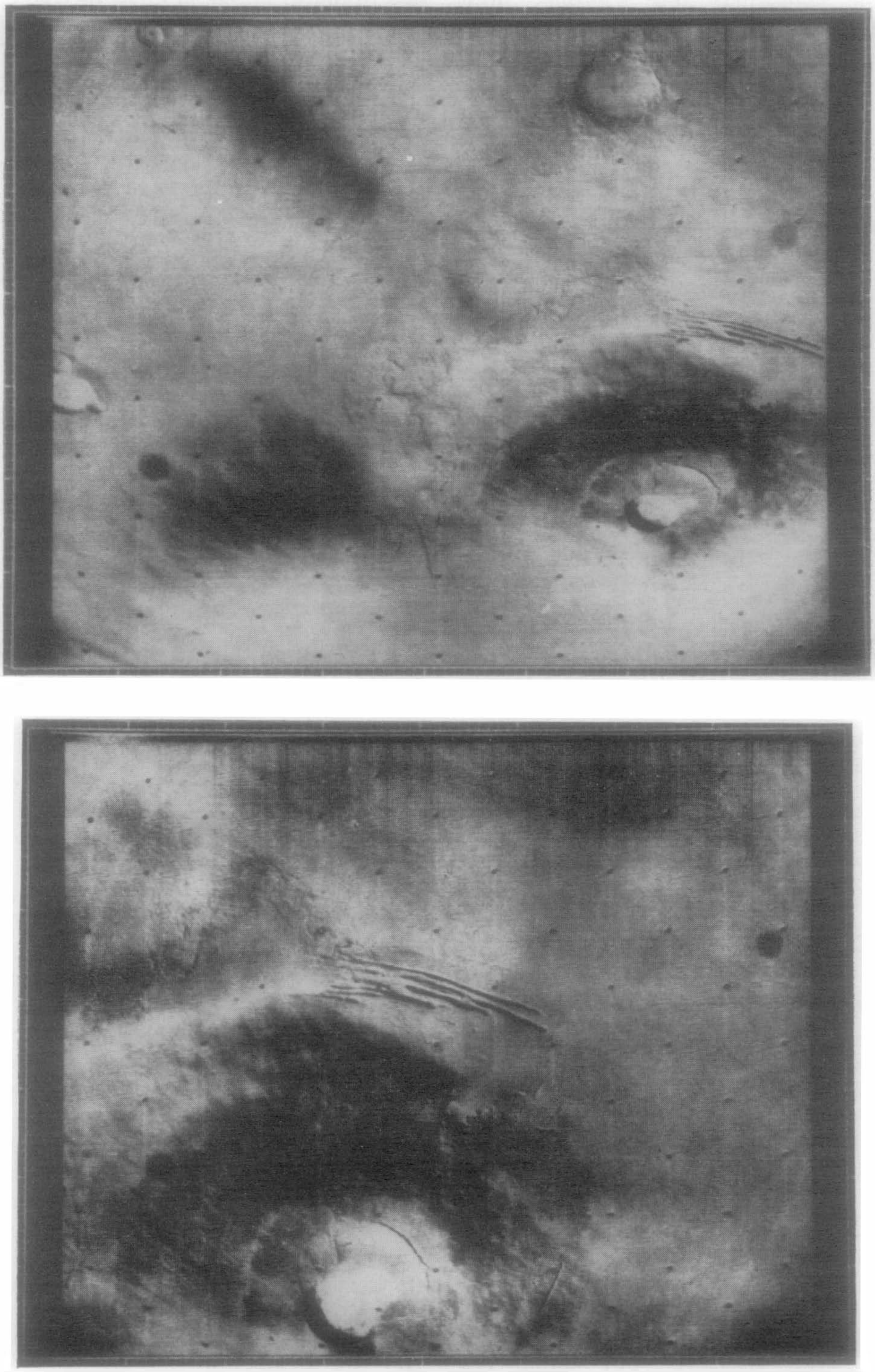

FIG. 8. Two general views of Pavonis Mons. Top: Revolution 152 (DAS 07039588) Bottom: Revolution 154 (DAS 07111198) The summit caldera is about 50 km across. North is at top, east to the right.

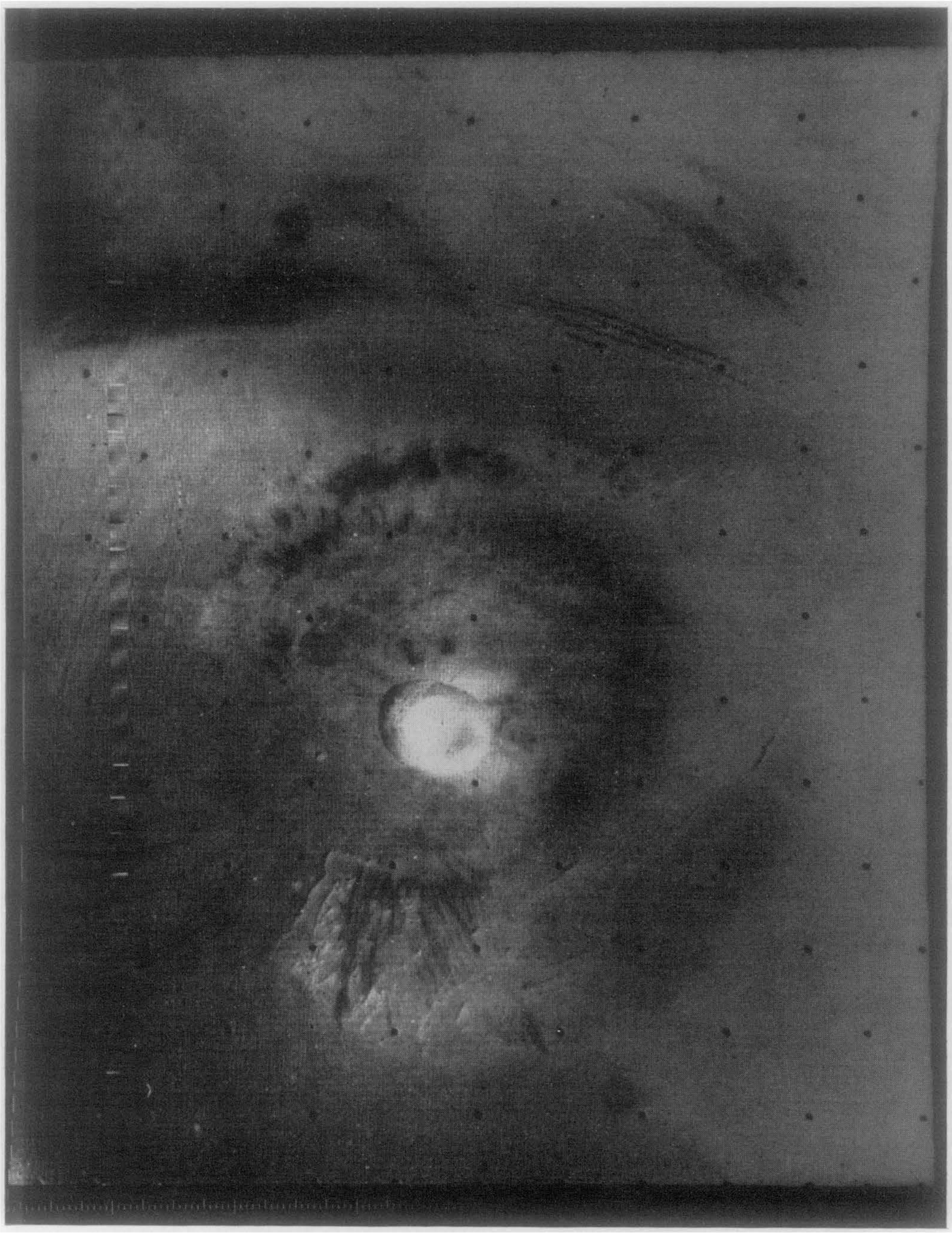

FIG. 9. General view of Pavonis Mons on Revolution 232. The appearance differs significantly from that in Fig. 8. First, the circumferential summit scarp, clearly visible in Fig. 8 is indistinct here. Second, note the intense dark radial markings around the base. These apparent changes are discussed in the text. (Summit caldera $\simeq$ 50 km. DAS 09916594).

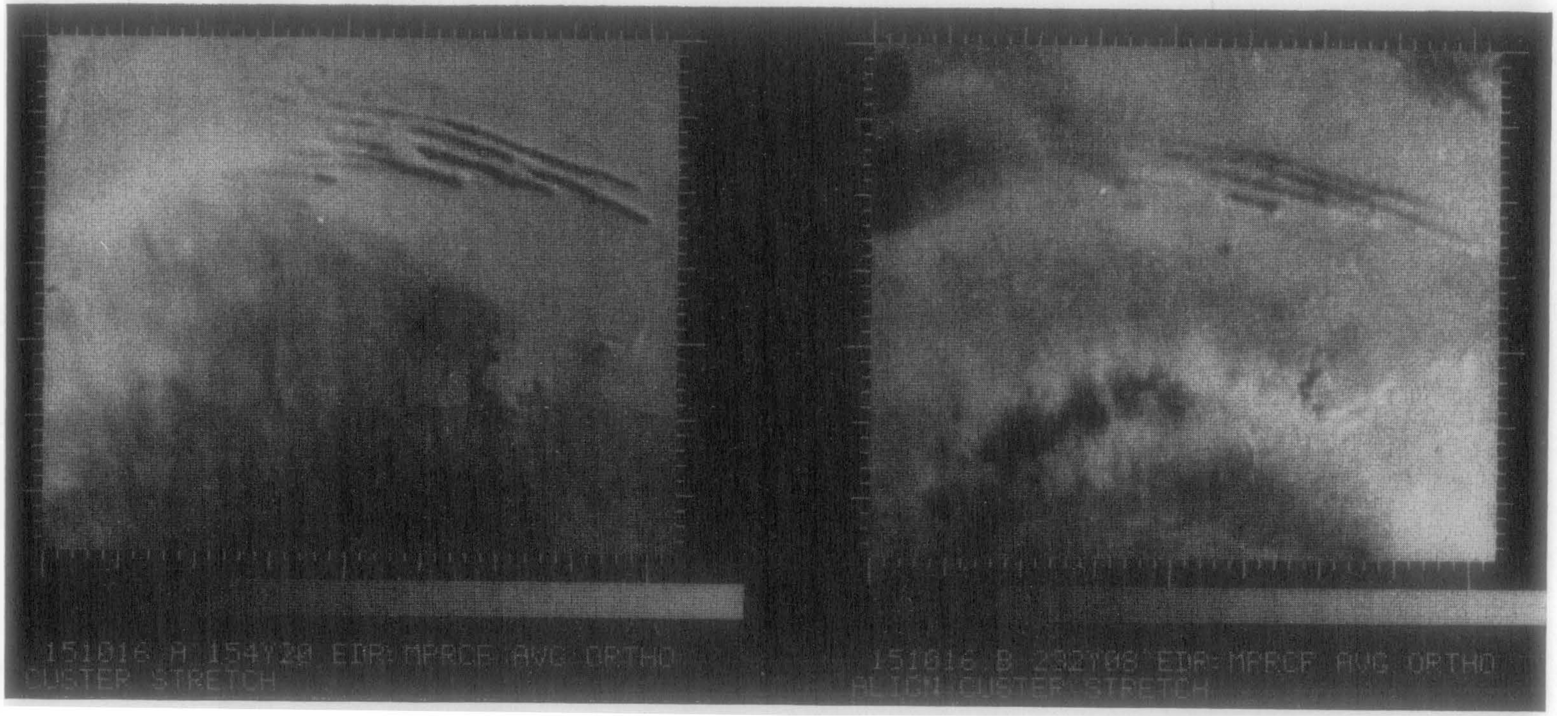

FIG. 10. Graben system and base of Pavonis Mons. Left: Revolution 154. Right: Revolution 232. Topographic detail is indistinct at right and several dark areas at the base of the volcano are surrounded by very bright patches—observations suggestive of clouds. However, it is argued in the text that the albedo changes may represent true surface changes, while the loss of topographic detail on the right can be attributed to different lighting conditions and increased transmission noise. Revolution 154. ($K = 1.20$; STN 151016).

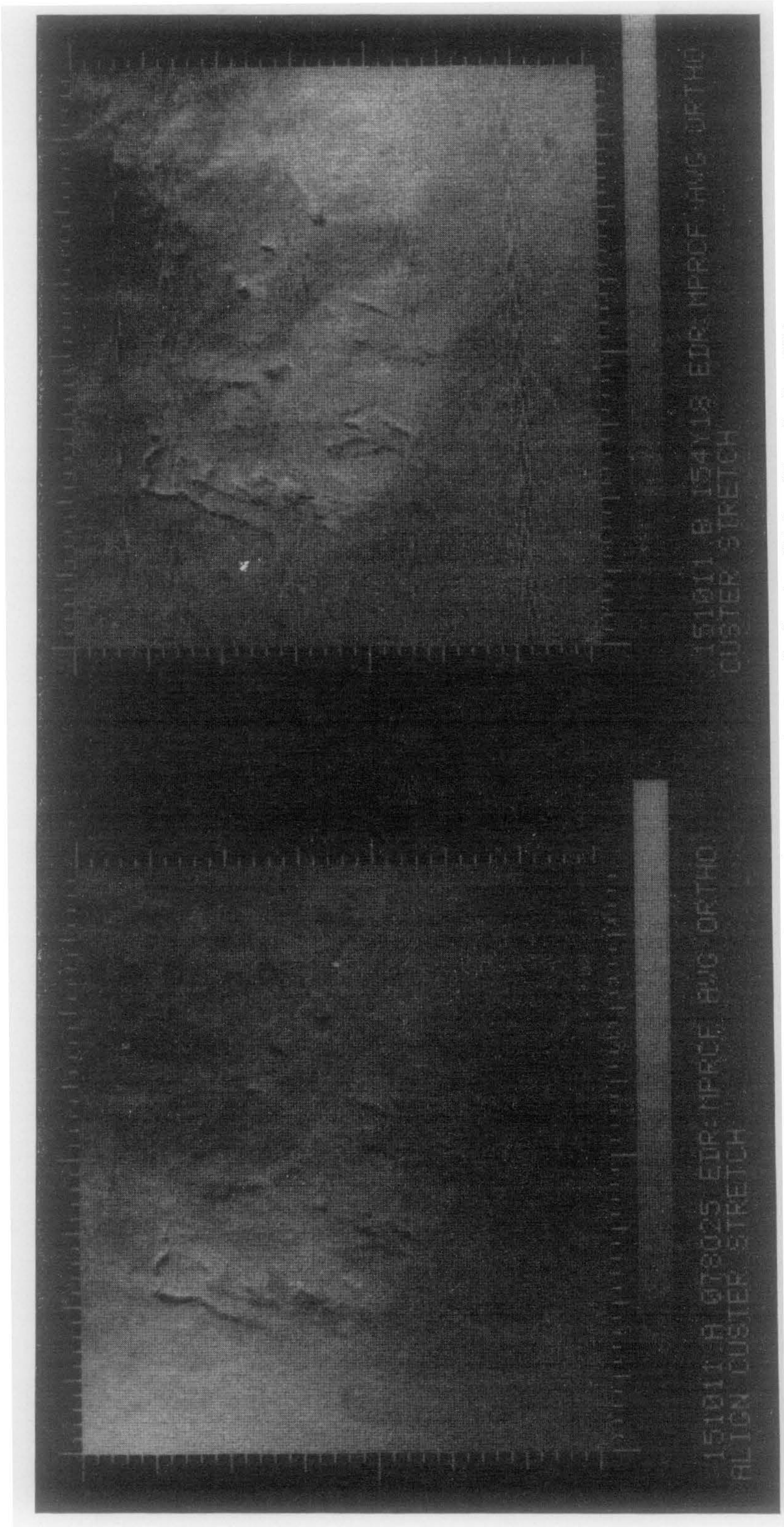

FIG. 11a. Eastern flanks of Pavonis Mons. Left: Revolution 78. Right: Revolution 154.

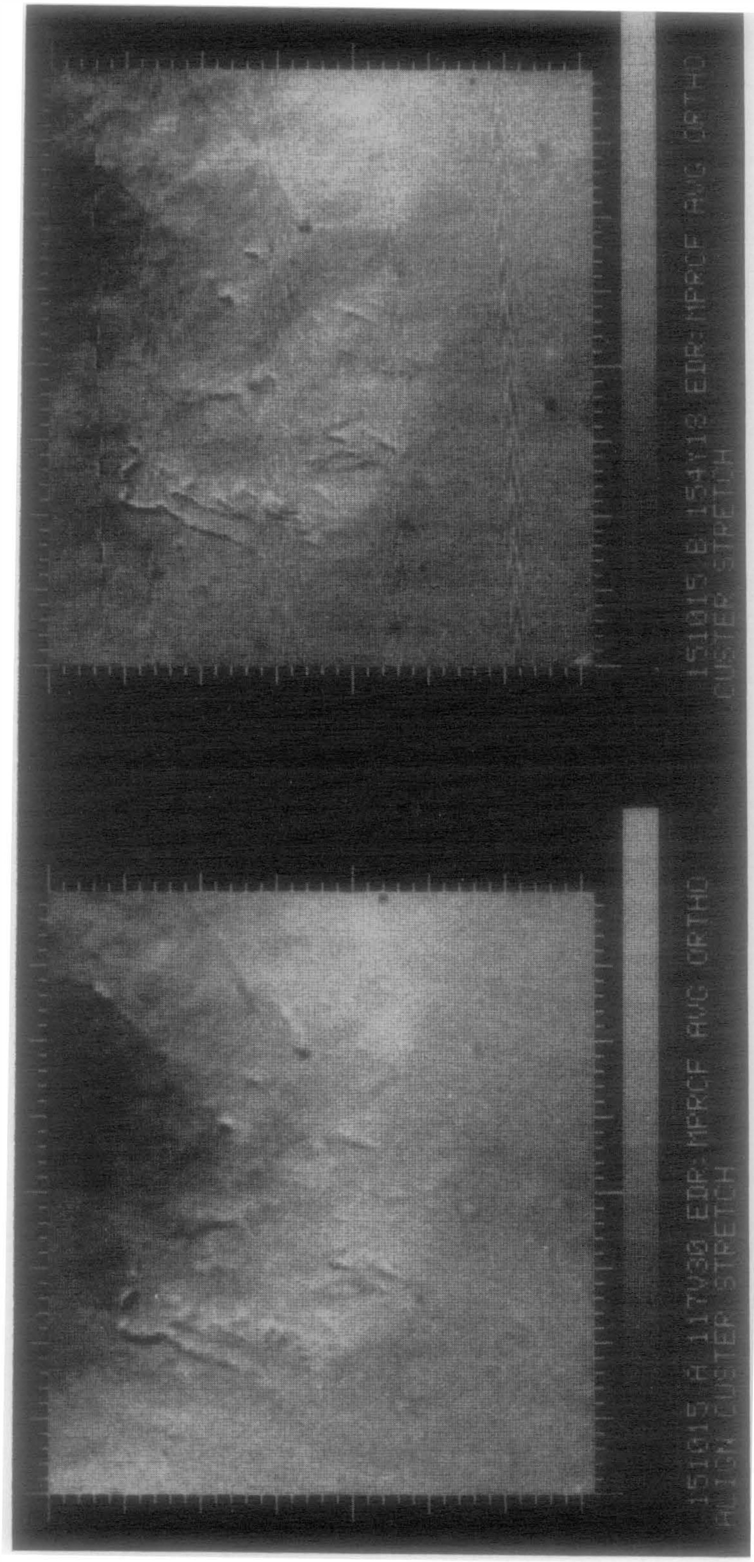

FIG. 11b. Left: Revolution 117. Right: Revolution 154.

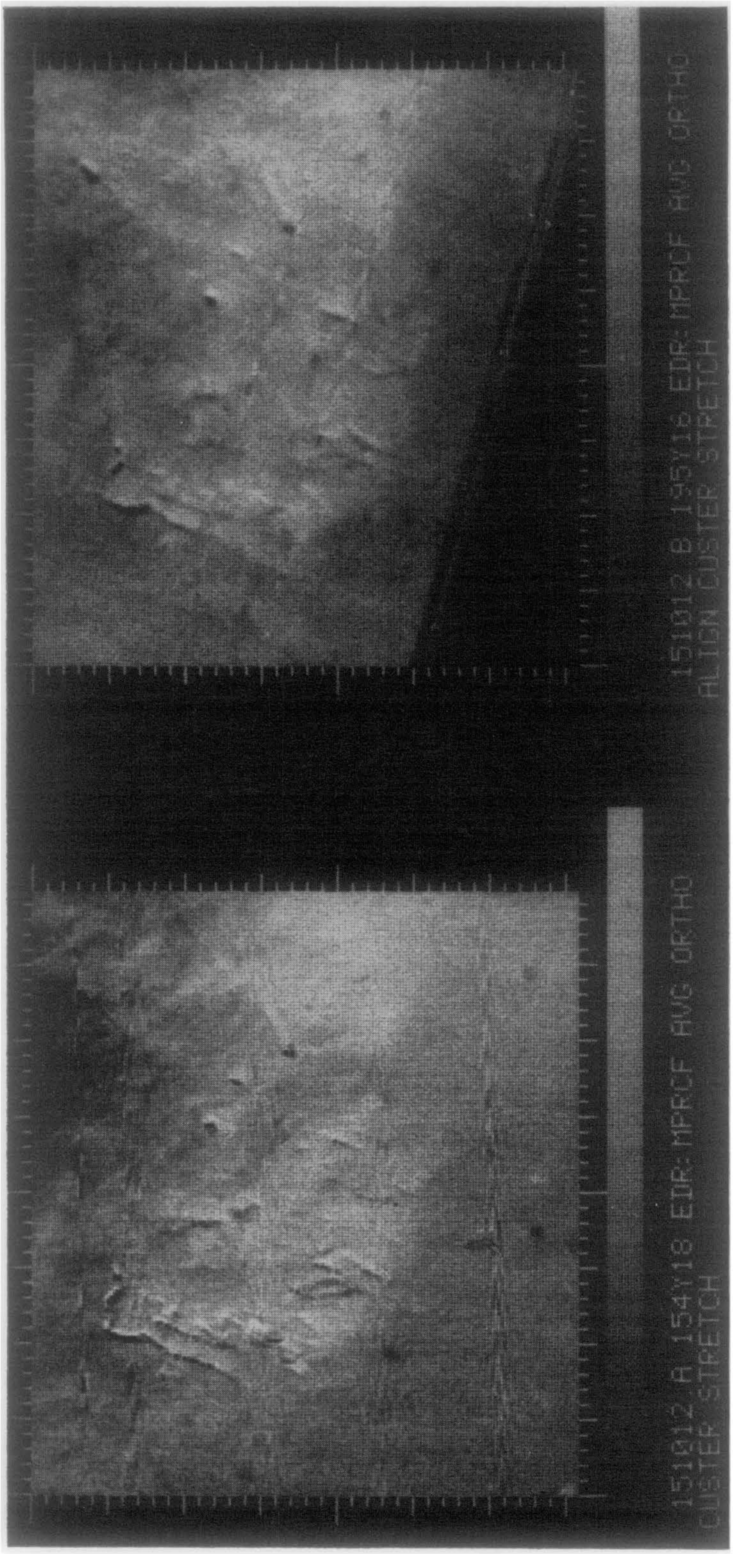

Fig. 11c. *Left:* Revolution 154. *Right:* Revolution 195.

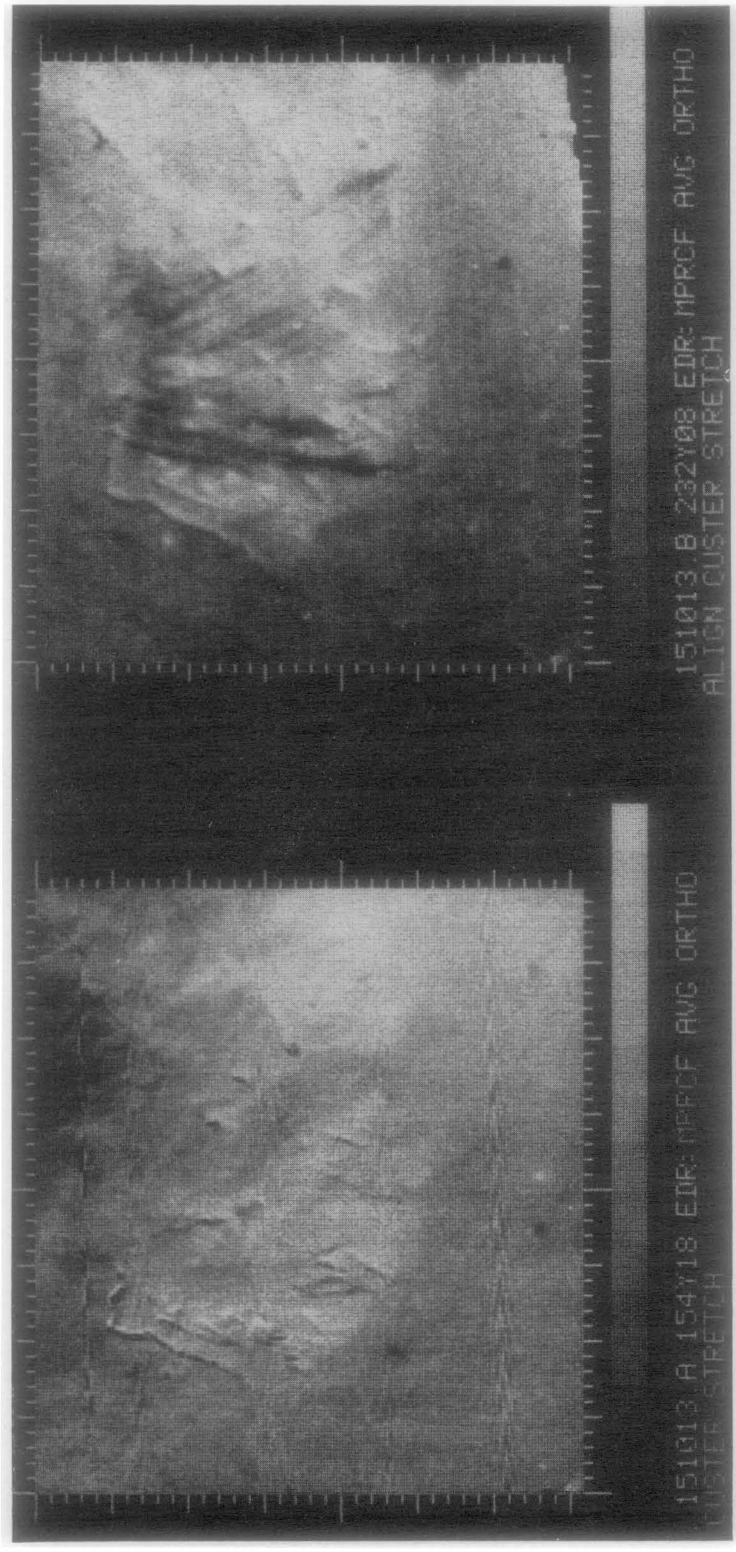

FIG. 11d. Left: Revolution 154. Right: Revolution 232.

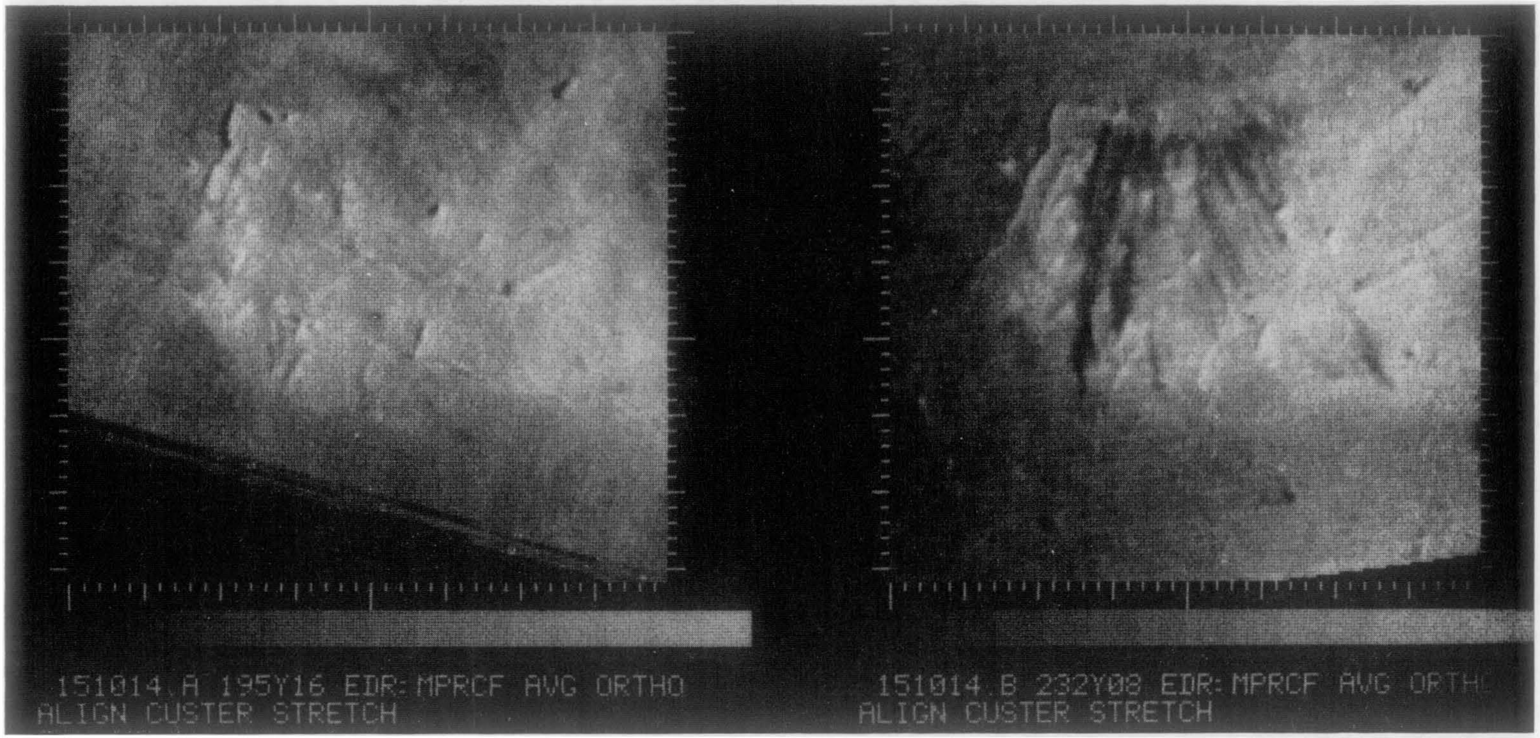

FIG. 11e. Left. Revolution 195. Right: Revolution 232. The appearance of the elongated radial dark albedo markings on Revolution 232 probably represents a surface change. Note the presence of at least one bright crater and streak near ($x = 150, y = 125$) ($K = 0.90$; STN 1510-15).

lacking high resolution photography of this area at the time in question, this possibility cannot be excluded with certainty. Many of the dark albedo features below the circumferential ridge are radial in aspect; a trend for bright and dark streaks in the Tharsis region to run downhill has already been noted (Sagan *et al.*, 1973). There are a number of similar radial dark streaks on the flanks of Ascraeus Mons, another large volcanic construct in Tharsis.

V. Conclusions

A range of albedo variations, in patches, from bright to dark, have been uncovered by Mariner 9 photography of the flanks of Pavonis Mons, a great shield volcano in Tharsis. The most striking variations occur near the summit caldera, at a pressure level estimated by a variety of independent techniques as about 1.5 mb. Using the lowest published estimate of the velocity contrast through the surface boundary layer, a value of the free stream velocity above the boundary layer of 110 m/s, or Mach 0.51, emerges. These albedo variations occur along radial wrinkle ridges. When account is made of local roughness, these velocities may be reduced by some tens of percent; on the other hand, if larger values of the velocity contrast are employed, free stream velocities approaching the speed of sound result. When circumferential slope winds are added to the general circulation winds (see Sagan *et al.*, 1971) wind velocities in this range are found; indeed, because of slope winds the highest velocity winds on Mars are anticipated precisely along the upper flanks of the great shield volcanoes.

This investigation suggests three areas deserving of further study:

(a) The effect of major topographic obstacles, such as Pavonis Mons, on boundary layer physics and the value of the temperature contrast through the boundary layer.

(b) Calculation of the expected magnitude of slope winds around equatorial volcanoes. This has not yet been done, because the slopes are too steep for the thermal wind equation to be valid, the latitudes of the volcanoes are too equatorial, and the lateral scale of these constructs falls between the ranges of applicability of the two appropriate approximations (see Gierasch and Sagan, 1971).

(c) Variable features observations of the upper reaches of Olympus Mons and other shield volcanoes by Viking and other future long-lived Mars orbiters.

Acknowledgments

We are grateful to Drs. M. Carr, P. Gierasch, C. Hord, and J. B. Pollack for helpful discussions. This research was supported by NASA Grant NGR 33-010-220.

References

Antoniadi, E. M. (1930). "La Planete Mars." Hermann, Paris.

Blasius, K. (1973). A study of Martian topography by analytic photogrammetry. *JGR* **78**, 4411.

Carr, M. (1973) Volcanism on Mars. *J. Geophys. Res.* **78**, 4049.

Conrath, B., Curran, R., Hanel, R., Kunde, V., Magire, W., Pearl, J., Pirraglia, J., Walker, J., and Burke, T. (1973). Atmospheric and surface properties of Mars obtained by infrared spectroscopy on Mariner 9. *J. Geophys. Res.* **78**.

Gierasch, P. and Goody, R. (1973). A model of a Martian great dust storm. *J. Atmos. Sci.* **30**, 169.

Gierasch, P. and Sagan, C. (1971). A preliminary assessment of Martian wind regimes. *Icarus* **14**, 312.

Greely, R., Inversen, J. D., Pollack, J. B., Udovich, N. and White, B. (1973). Wind tunnel studies of Martian aeolian processes. NASA Technical Memorandum (NASA TMX-62297).

Hartmann, W. K. (1973). Martian cratering. IV. Mariner 9 initial analysis of cratering chronology. *J. Geophys. Res.* **78**, 4096.

Hess, S. (1973). Martian winds and dust clouds. *Planet. Space Sci.* **21**, 1549.

Hord, C., Simmons, K., and McLaughlin, L. (1974). Mariner 9 ultraviolet experiment: pressure–altitude measurements on Mars. *Icarus* **21**, 292–302

Kliore, A. J., Fjeldbo, G., Seidel, B. L., Sykes, J. J. and Woiceshyn, P. M. (1973). S-Band radio occultation measurements of the atmosphere and topography of Mars with

Mariner 9. Extended mission coverage of polar and intermediate latitudes. *J. Geophys. Res.* **78**, 4331.

Leovy, C., Briggs, G., Young, A. T., Smith, B. A., Pollack, J., Shipley, E. and Wildey, R. (1972). Mariner 9 television experiment: progress report on studies of the Mars atmosphere. *Icarus* **17**, 373–393.

Levinthal, E. C., Green, W. B., Cutts, J. A., Jahelka, E. D., Johansen, R. A., Sander, M. J. Seidman, J. B., Young, A. T. and Soderblom, L. A. (1973). Mariner 9 image processing and products. *Icarus* **18**, 75–101.

Macdonald, G. A. (1972). "Volcanoes." Prentice-Hall. Englewood Cliffs, New Jersey.

McCauley, J. F., Carr, M. H., Cutts, J. A., Hartmann, W. K., Masursky, H., Milton, D. J., Sharp, R. P., and Wilhelms, D. E. (1972). Preliminary Mariner 9 report on the geology of Mars. *Icarus* **17**, 289–327.

Masursky, H., Batson, R. M., McCauley, J. F., Soderblom, L. A., Wildey, R. L., Carr, M. H., Milton, D. J., Wilhelms, D. E., Smith, B. A., Kirby, T. B., Robinson, J. C., Leovy, C. B., Briggs, G. A., Duxbury, T. C., Acton, C. H., Murray, B. C., Cutts, J. A., Sharp, R. P., Smith, S., Leighton, R. B., Sagan, C., Veverka, J., Noland, M., de Vaucouleurs, G., Davies, M., and Young, A. T. (1972). Mariner 9 television reconnaissance of Mars and its satellites: Preliminary results. *Science* **175**, 294–304.

Parkinson, T. D., and Hunten, D. M. (1973). CO_2 distribution on Mars. *Icarus* **18**, 29.

Quam, L., Tucker, R., Eross, B., Veverka, J. and Sagan, C. (1973). Mariner 9 picture differencing at Stanford. *Sky and Telescope* **46**, 84–87.

Sagan, C., and Veverka, J. (1974). Models of Martian albedo variations. In preparation.

Sagan, C. and Pollack, J. B. (1967). A windblown dust model of Martian surface features and seasonal changes. Smithsonian Astrophysical Observatory Special Report 255.

Sagan, C. and Pollack, J. B. (1969). Windblown dust on Mars. *Nature* **223**, 791.

Sagan, C., Veverka, J., and Gierasch, P. (1971). Observational consequences of Martian wind regimes. *Icarus* **15**, 253.

Sagan, C., Veverka, J., Fox, P., Dubisch, R., Lederberg, J., Levinthal, E., Quam, L., Tucker, R., Pollack, J. B., and Smith, B. A. (1972). Variable features on Mars: Preliminary Mariner 9 results. *Icarus* **17**, 346–372.

Sagan, C., Veverka, J., Fox, P., Dubisch, R., French, R., Gierasch, P., Quam, L., Lederberg, J., Levinthal, E., Tucker, R., Eross, B., and Pollack, J. B. (1973). Variable features on Mars. 2. Mariner 9 global results. *J. Geophys. Res.* **78**, 4163–4196.

Veverka, J., Sagan, C., Quam, L., Tucker, R., and Eross, B. (1974). Variable features on Mars. III. Comparison of Mariner 1969 and Mariner 1971 photography. *Icarus*, in press.